



## Metabolomic Profiling of *Streptomyces griseorubens* with the Evaluation of their Antioxidant and Anticancer Potentialities



Mahmoud Nazeeh<sup>1</sup>; Mostafa A. Asmaey<sup>2\*</sup>; Ahmed M. El-Adly<sup>1</sup> and Magdy M. Afifi<sup>3</sup>

<sup>1</sup>Botany and Microbiology Department, Faculty of Science, Al-Azhar University, 71524, Assiut, Egypt

<sup>2</sup>Department of Chemistry, Faculty of Science, Al-Azhar University, Assiut Branch, 71524, Assiut, Egypt

<sup>3</sup>Botany and Microbiology Department, Faculty of Science, Al-Azhar University, Nasr City, Cairo 11884, Egypt.

### Abstract

*Streptomyces* species have long been recognized as prolific producers of bioactive compounds with therapeutic potential. In this study, our focus rested on the isolation and identification of *Streptomyces griseorubens* (AUMC B-519) among a diverse collection of 94 different actinomycete isolates obtained from several soil sites across Egypt. Our exploration was performed through the assessment of pigment production among these isolates. To gain deeper insights into the chemical composition of *S. griseorubens*; we employed metabolomic profiling using gas chromatography-mass spectrometry (GC-MS) and ultra-performance liquid chromatography-mass spectrometry (UPLC-MS) hyphenated with quadrupole-time-of-flight tandem mass spectrometry (QTOF-MS). This comprehensive metabolomic analysis provided a detailed view of the metabolites present in the extract, allowing us to identify key compounds responsible for the observed bioactivities. The GC-MS analysis enabled the detection of 21 compounds while, the UPLC-MS afforded 44 compounds, including a wide range of secondary metabolites, such as glycosides, carboxylic acid derivatives, lipids of triterpene derivatives, alkaloids, and flavonoids. Most of the identified compounds were described for the first time from this strain. In parallel, we assessed the antioxidant and anticancer potentialities of the ethyl acetate extract. The extract revealed restrained anticancer activity against MCF7 cell line coupled with a mild effect against 1, 1-diphenyl-2-picryl hydrazyl (DPPH) scavenging, exhibiting MIC values of 343.34 and 55.97 µg/mL, respectively. This study unequivocally underscores the potential of *S. griseorubens* as a valuable source of bioactive compounds. Moreover, the metabolomic profiling approach revealed the intricate chemical diversity within the extract, shedding light on the complex metabolic pathways and compounds produced by this *Streptomyces* strain. These findings contribute to our understanding of *S. griseorubens* pharmacological properties and pave the way for further investigations into its biomedical applications.

**Keywords:** Anticancer activity; Antioxidant activity; Metabolomics; UPLC-MS/MS; *Streptomyces griseorubens*

### 1. Introduction

The exploration of natural products from microbial sources has garnered immense interest in drug discovery due to their vast chemical diversity and potential therapeutic applications [1, 2]. *Streptomyces* species, commonly found in soil ecosystems, have

been a prolific source of bioactive secondary metabolites, including antibiotics, antioxidants, and anticancer agents. Their ability to produce an array of structurally diverse compounds makes them a promising target for drug discovery efforts. *Streptomyces griseorubens*, a member of the *Streptomyces* genus, is known for its versatile metabolic capabilities. Previous investigations have documented the production of diverse bioactive

\*Corresponding author e-mail: asmaey.mostafa.2142@azhar.edu.eg

Received date 30 November 2023; revised date 04 February 2024; accepted date 06 February 2024

DOI: [10.21608/EJCHEM.2024.250016.8929](https://doi.org/10.21608/EJCHEM.2024.250016.8929)

©2024 National Information and Documentation Center (NIDOC)

compounds by *S. griseorubens*, including antifungal agents, anti-inflammatory compounds, and enzyme inhibitors [3-5]. However, the antioxidant and anticancer potential of this particular strain remains relatively unexplored. In this study, we isolated *S. griseorubens* from soil samples, utilizing selective culture techniques and molecular identification methods. The crude extract obtained through ethyl acetate extraction was subjected to evaluation for its antioxidant activity, utilizing established assays to measure scavenging capacity against free radicals [6]. Additionally, we investigated the anticancer potential of the ethyl acetate crude extract against the MCF7 cancer cell line, assessing its cytotoxic effects, and cell proliferation inhibition. To gain deeper insights into the chemical composition and identify potential bioactive molecules, we employed metabolomics profiling techniques, including gas (GC-MS) and (UPLC-MS) [7]. The combined utilization of these analytical approaches allows for a comprehensive analysis of the extract's metabolites, enabling the identification and characterization of various secondary metabolites [8]. The findings from this study provide valuable data on the antioxidant and anticancer activities of *S. griseorubens* ethyl acetate crude extract, highlighting its potential as a rich source of bioactive compounds. Furthermore, the metabolomic profiling approach elucidates the intricate chemical diversity within the extract, facilitating the identification of key metabolites responsible for its pharmacological properties. These findings contribute to our understanding of *S. griseorubens*' therapeutic potential and open avenues for further research in the field of natural product drug discovery.

## 2. Materials and Methods

### 2.1. Sample Collection and Isolation of Strain

Soil samples were gathered from various localities within the Awlad Saqr region in Alsharkia governorate, Egypt. Soil samples were collected from a depth of 8-10 cm below the surface, placed in sterilized polyethylene bags, and brought to the laboratory for subsequent experiments [9]. One gram of soil was mixed with sterilized distilled water and subjected to agitation in a rotary shaker for 10 minutes,

followed by serial dilution. The samples, after dilution, were evenly distributed across plates using different types of media, including starch nitrate agar (SNA)[10] and then incubated for 7 days at 37°C [11]. The resulting isolated actinomycete cultures were further purified on fresh media and stored in a biochemical oxygen demand incubator.

### 2.2. Identification of the Isolated Actinomycete

#### 2.2.1. Morphological Identification

The isolated strain was inoculated onto Luria Bertani, M1 medium (soluble starch 20 g/L, KNO<sub>3</sub> 1.0 g/L, KH<sub>2</sub>PO<sub>4</sub> 0.5 g/L, NaCl 0.5 g/L, FeSO<sub>4</sub>.7H<sub>2</sub>O 0.01 g/L, MgSO<sub>4</sub>.7H<sub>2</sub>O 0.05 g/L, agar 20 g/L, and natural seawater 1.0 L, pH 7.2–7.6) in agar plate and cultured for 14 days to observe the morphology of the isolate. Samples for scanning electron microscopy (SEM) were prepared by the insertion method. Briefly, the isolate was cultured on a solid medium, and sterilized coverslips, frozen at -80 °C for 24 h and then lyophilized for 48 h to remove water. Finally, the coverslips were sprayed with gold, and strain morphology was assessed by SEM (Fig. 1) [4]. The morphology of the selected isolate was found spore-bearing hyphae with an entire spore chain along with substrate and areal mycelium under light and scanning electron microscope [12]. A characteristic of the spore-bearing hyphae and spore chains was determined by the direct microscopic examination of the culture. Adequate magnification was used to establish the presence or absence of spore chains. Different biochemical tests such as catalase, urease, pectinase, starch hydrolysis, casein hydrolysis, cellulose hydrolysis, and gelatin hydrolysis, along with the utilization of different sugars and nitrogen sources were performed [13].

#### 2.3. Molecular Identification and Phylogenetic Analysis

The isolated strain was cultured on nutrient agar medium [14] and incubated at 28 °C for 48 hours before transferring to the Molecular Biology Research Unit, at Assiut University. DNA extraction was performed using a Patho-gene-spin DNA/RNA extraction kit provided by Intron Biotechnology Company, Korea. The extracted DNA samples were sent to SolGent Company, Daejeon South Korea for polymerase chain reaction (PCR) and gene

sequencing. PCR was performed using two universal primers namely 27F (5'-

AGAGTTTGATCCTGGCTCAG-3') and 1492R (5'-GGTTACCTTGTT ACGACTT-3').

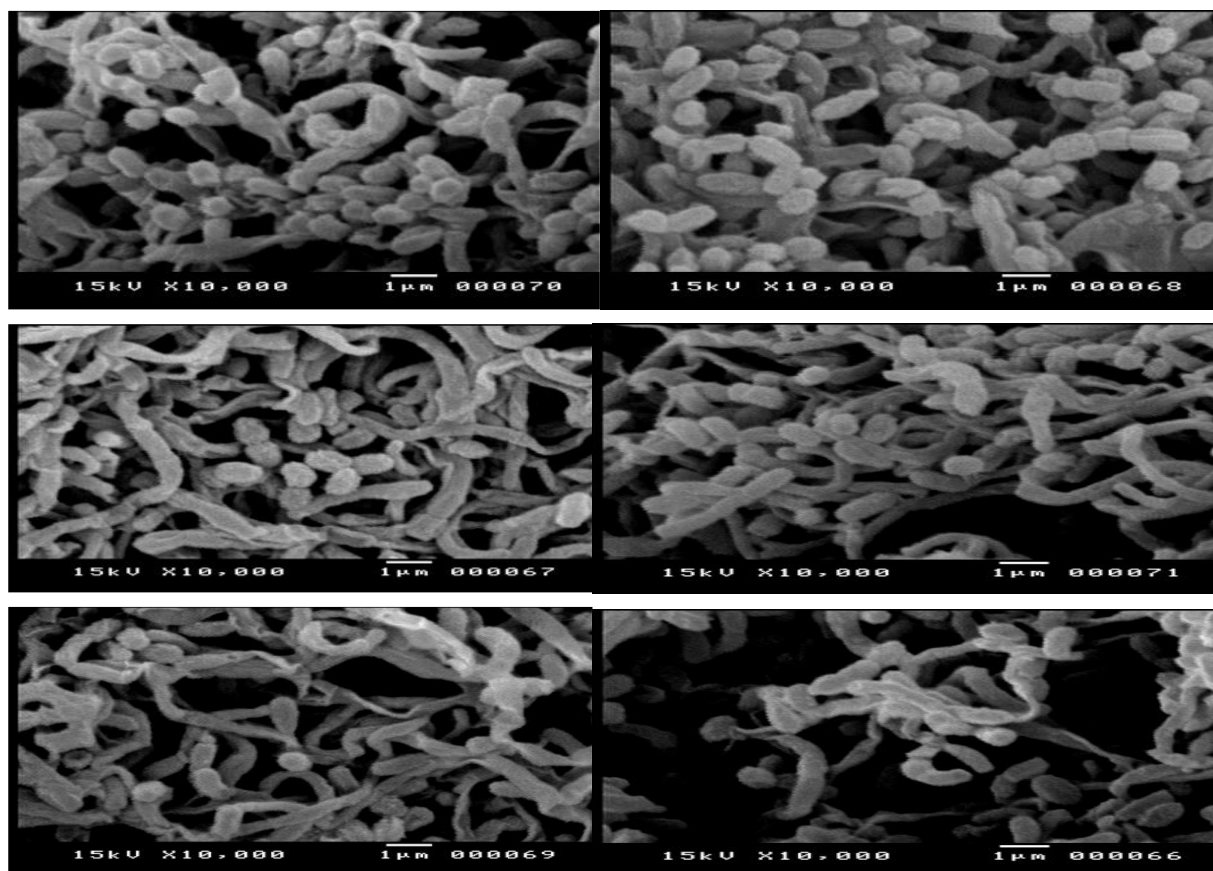


Fig. 1. Scanning electron microscopy (SEM) for morphological identification of *S.griseorubens*

The purified PCR products (amplicons) were reconfirmed using a size nucleotide marker (100 base pairs) by electrophoreses on 1% agarose gel. Purified amplicons were sequenced in the sense and antisense directions using 27F and 1492R primers with the incorporation of dideoxynucleotides (dd NTPs) in the reaction mixture [15]. Sequences were further analyzed using the Basic Local Alignment Search Tool (BLAST) from the National Center of Biotechnology Information (NCBI) website. Phylogenetic analysis of sequences was done using MegAlign (DNA Star) software version 5.05.

#### 2.4. Optimization of culture medium

The production of crude extract was evaluated in basal medium composed of starch-nitrate medium It contains (g/L): soluble starch, 20.0; NaNO<sub>3</sub>, 2.0; K<sub>2</sub>HPO<sub>4</sub>, 1.0 KCl, 0.5; MgSO<sub>4</sub>.7H<sub>2</sub>O, 0.5;

CaCO<sub>3</sub>.2H<sub>2</sub>O, 2.0 and distilled water up to 1000 mls. The pH of the medium was adjusted at pH 7 before sterilization [16]. The pigment production by strain *S. griseorubens* was evaluated at various pH in comparison to 3,4,5,6,7,8,9,10 and 11 for 8 days and optical density was recorded at 480 nm [17]. Different carbon sources including lactose, glucose, fructose, starch, sucrose, dextrose, and maltose were tested. Also, nitrogen sources including sodium nitrate, ammonium nitrate, casein, urea, arginine, sodium nitrite, and ammonium sulfate were added to the basal medium at 1.0% (v/v) of concentration. The spore suspension of 5 ml ( $5 \times 10^9$  spores/mL) was added to a 50 mL basal medium supplemented with various carbon and nitrogen sources and incubated on a rotary shaker at 37 °C for 8 days. The inorganic salt medium without carbon and nitrogen sources served as control. The pigment extract was dissolved in a 0.5 M NaOH solution for spectroscopic examination. This solution was then analyzed using a UV-visible

spectrophotometer, which operates at near-infrared wavelengths ranging from 200 to 800 nm. A 0.5 M NaOH solution served as the blank for this analysis [16]. The biomass consisting of bioactive metabolite was recorded at 480 nm (optical density) [18].

### 2.5. Fermentation and extraction of crude extract

The strain *S. griseorubens* was cultivated on starch nitrate agar medium under aseptic conditions and incubated at 37 °C for 7 days [19]. After the incubation was complete, spores from freshly grown slant were scrapped and inoculated into starch-nitrate broth medium at 150 rpm for 7 days. To extract the crude 100 mL of sterilized starch nitrate broth medium was supplemented with starch and ammonium nitrate as carbon and nitrogen sources, respectively and incubated at 37 °C for 8 days.

The obtained liquid broth was extracted (3 x 1L) using ethyl acetate. The solvent was then evaporated under reduced pressure until complete dryness, resulting in the production of 0.165 gm of extract. This extract was subsequently employed for biological investigations. Moreover, for a comprehensive metabolomic analysis, the extract underwent further fractionation and defatting using cyclohexane (C-Hex). The resulting C-Hex fraction, as well as the defatted (polar fraction), were carefully kept at 4 °C.

### 2.6. Metabolomic studies of *S. griseorubens* extract

#### 2.6.1. GC-MS analysis of the nonpolar fraction

The analysis of (C-Hex) fraction via GC-MS was conducted using a Trace GC-TSQ mass spectrometer (Thermo Scientific, Austin, TX, USA) equipped with a direct capillary column TG-5MS (30 m x 0.25 mm x 0.25 µm film thickness). The column temperature was initially set at 50 °C, then increased at a rate of 5°C/min to reach 250 °C, where it was maintained for 2 minutes. Subsequently, it was further increased at a rate of 30 °C/min to the final temperature of 300 °C and held for 2 minutes. The injector and MS transfer line temperatures were maintained at 270 °C and 260 °C, respectively. Helium served as the carrier gas with a constant flow rate of 1 ml/min. A solvent delay of 4 minutes was implemented, and 1 µl diluted samples were

automatically injected using an Autosampler AS1300 coupled with GC in the split mode. Electron Ionization (EI) mass spectra were acquired at an ionization voltage of 70 eV over the range of  $m/z$  50–650 in full scan mode. The ion source temperature was set at 200 °C, adhering to the methodology outlined by Abd El-Kareem and coauthors [17].

The identification of the compounds was accomplished by comparing their mass spectra with the reference spectra available in the WILEY 09 and NIST 14 mass spectral databases.

#### 2.6.2. UPLC-MS analysis of the polar fraction

In situations where many components exhibit comparable polarity, UPLC stands as a contemporary technology that presents an innovative approach to liquid chromatography for the separation of intricate mixtures. This specific chromatographic technique delivers superior resolution compared to HPLC, operating with increased speed and reduced solvent consumption. UPLC achieves this efficiency by employing a narrower column packed with particles, usually less than 2 micrometres in diameter. The rapid characterization of components is significantly improved when a mass spectrum of each eluting component from the LC column can be recorded. Typically, ESI-MS and LC are interconnected to facilitate effective online LC/MS.

#### Instrumentation and Data Acquisition Method

The defatted extract of *S. griseorubens* was injected into an Axion AC system from Kyoto, Japan. This system was equipped with an autosampler, an In-Line filter disks precolumn (0.5 µm x 3.0 mm, Phenomenex, USA), and an Xselect HSS T3 C18 column (2.5 µm x 2.1 mm x 150 mm) from Waters Corporation, Milford, MA, USA. The column was maintained at a temperature of 40 °C, and the flow rate was set at 300 µL/min. The separation process utilized a mobile phase comprising two solutions. In the positive mode, solution (A) consisted of 5 mM ammonium formate in 1% methanol, with the pH adjusted to 3.0 using formic acid. In the negative mode, solution (B) was composed of acetonitrile 100%, and solution (C) contained 5 mM ammonium formate in 1% methanol, with the pH adjusted to 8.0 using ammonium hydroxide. For mass spectrometry (MS), the analysis was conducted using the Triple

TOF™ 5600+ system equipped with a Duo-Spray™ source, operating in the electrospray ionization (ESI) mode by AB SCIEX, located in Concord, Canada. Following each scan, the system selected the top 15 most intense ions for acquiring MS/MS fragmentation spectra, as outlined in references [18, 19].

#### Data Processing

The MS-DIAL 4.6 software, developed in Yokohama, Kanagawa, Japan, was utilized for a comprehensive non-targeted analysis of small molecules in the sample. Depending on the particular acquisition mode, either the ReSpect-positive database (consisting of 2737 records) or the ReSpect-negative database (comprising 1573 records) was employed as the reference source.

#### 2.7. In vitro Biological Assays

##### 2.7.1. Antioxidant Activity

The free radical scavenging activity of *S. griseorubens* was assessed using the (DPPH) assay, following the methodology [6].

##### 2.7.2. Anticancer Activity using MTT Protocol

The anticancer and cell proliferation studies of different concentrations from *S. griseorubens* crude extract were tested against MCF-7 cancer cells (human breast carcinoma) via the MTT assay method [20].

### 3. Results

Among 94 actinomycete isolates, only five actinomycetes were chosen according to pigment-producing ability. However, based on the diffusion ability, *S. griseorubens* was selected as the most promising isolate for further study. The pigment-producing ability of *S. griseorubens* was tested on solid as well as in broth media [24]. The morphological observations were recorded on the basis of the International *Streptomyces* Project (ISP) and revealed the abundant growth of aerial and vegetative mycelium on starch nitrate medium, yeast extract-malt extract medium (ISP-2) and oatmeal agar (ISP-3) [25]. The strain *S. griseorubens* produced an

orange color as reverse pigment on starch nitrate medium as well on ISP-2. Additionally, *S. griseorubens* showed abundant growth in carbon sources including starch, lactose, dextrose, mannitol, maltose, and fructose while starch showed the best carbon sources (Fig. 7) and ammonium nitrate represented the best nitrogen source (Fig. 5). Moreover, Table 1, showed that *S. griseorubens* hydrolyzed catalase, starch, urea, and gelatin, however, it was not capable of degrading pectine. The optimum incubation temperature was found to be at 37 °C (Fig. 4). Finally, the pigment production was found to be highest at pH 5 on the 8<sup>th</sup> day of the incubation period according to Fig. 6.

To taxonomically classify the AUMC B-519 strain, its genetic sequence was amplified using the polymerase chain reaction (PCR), subsequently sequenced, and subjected to analysis through a BLAST-based methodology. The phylogenetic examination of the 16S rRNA gene sequence demonstrated a high degree of similarity between AUMC B-519 and *S. griseorubens*, with a 99.79% match.

This correlation was further confirmed by the neighbor-joining-based phylogenetic tree shown in Fig. 2. Additionally, the gene sequence has been officially recorded in the GenBank database under accession number [OQ909101](#).

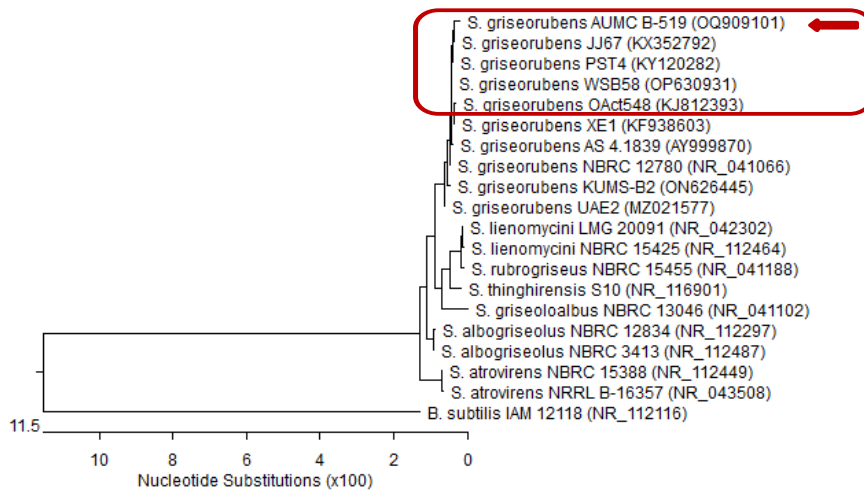
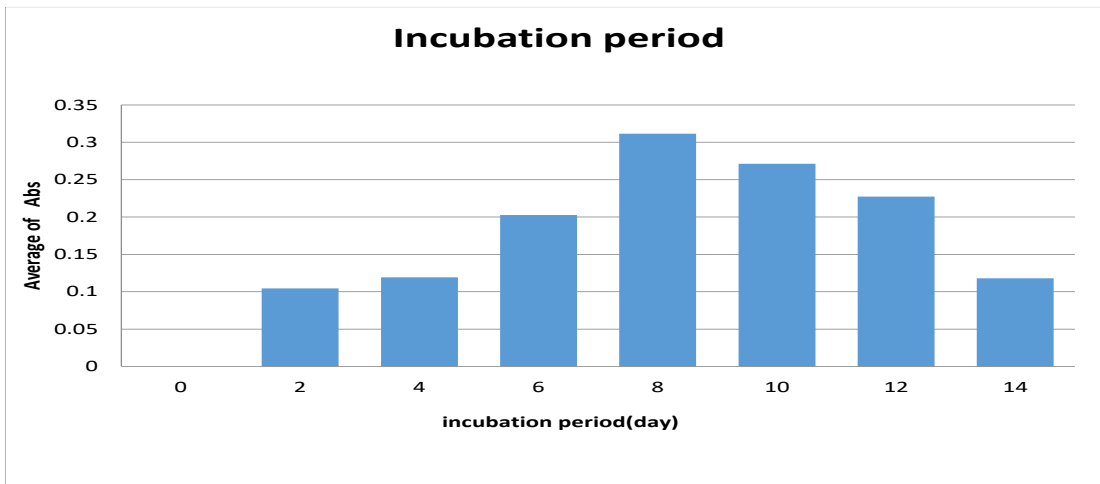
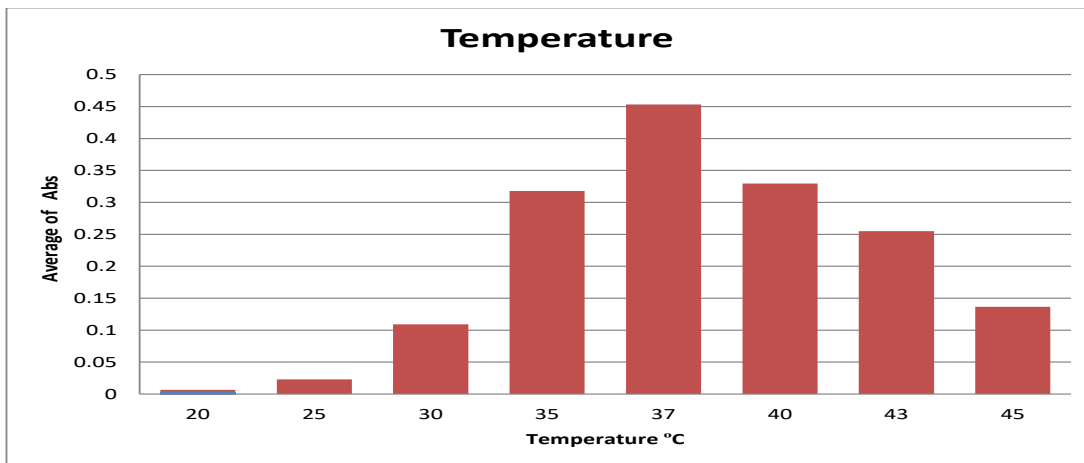


**Fig. 2.** Neighbor-joining phylogenetic tree of AUMC B-519 based on 16S rRNA gene sequences, showing its close relationship to *Streptomyces* species. *Bacillus subtilis* is included in the tree as an outgroup strain, B. = *Bacillus*, S. = *Streptomyces*.



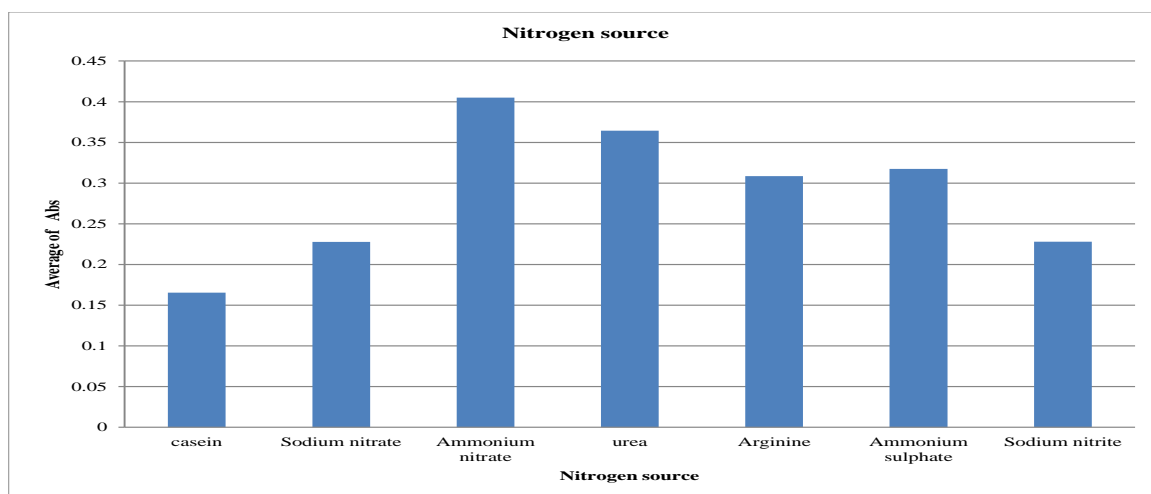
Abs = Absorbance

**Fig. 3.** Effect of different incubation periods on pigment production by *S. griseorubnes*



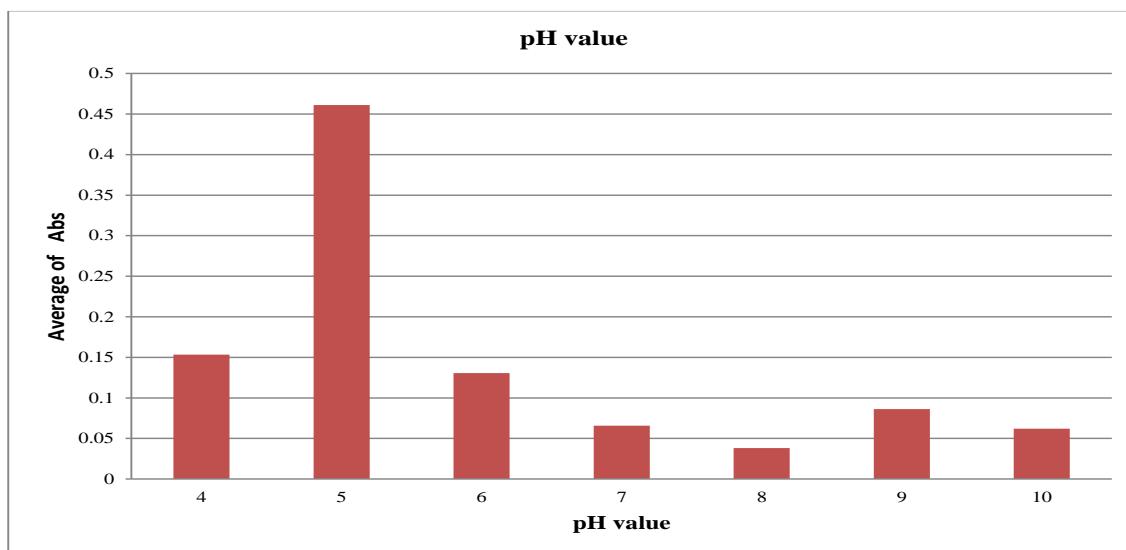
Abs = Absorbance

**Fig. 4.** Effect of different temperatures on pigment production by *S. griseorubnes*



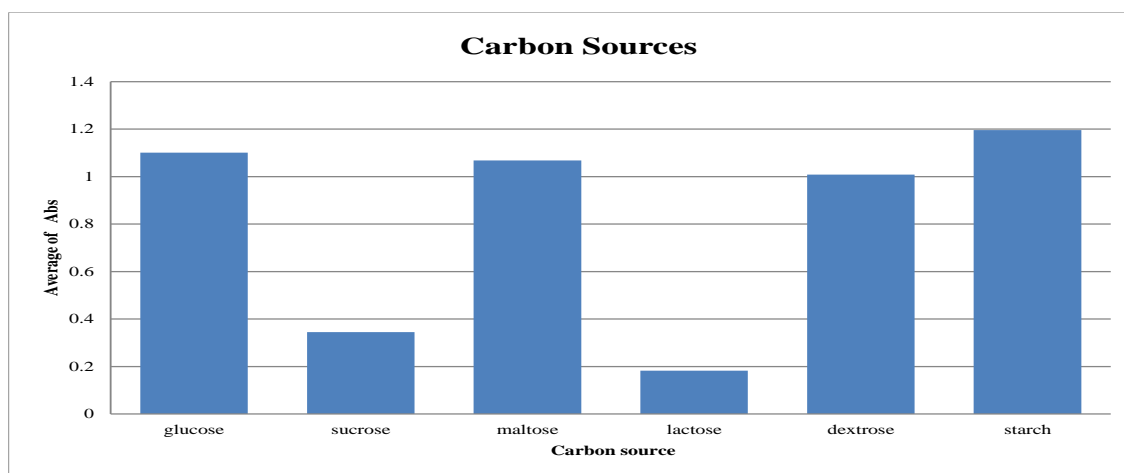
Abs =Absorbance

**Fig. 5.** Effect of different nitrogen sources on pigment production by *S. griseorubnes*



Abs =Absorbance

**Fig. 6.** Effect of different pH values on pigment production by *S. griseorubnes*



Abs =Absorbance

**Fig. 7.** Effect of different carbon sources on pigment production by *S. griseorubnes*

**Table 1.** Biochemical tests of *S.griseorubnes* strain

Biochemical Tests	Results
Catalase	+ve
Starch hydrolysis	+ve
Gelatin hydrolysis	+ve
Pectin hydrolysis	-ve
Urea hydrolysis	+ve
Carboxymethyl cellulose hydrolysis	+ve

+ve: Positive, -ve: Negative

### 3.1. Metabolomic studies

#### 3.1.1. Investigation of C-Hex fraction by GC/MS

A total of 21 compounds were identified from the non-polar fraction of *S. griseorubnes* through GC-MS ( Fig. 8 and

Table 2). The major components were bis(2-ethylhexyl) phthalate (DEHP) (MW:390, MF: C<sub>24</sub>H<sub>38</sub>O<sub>4</sub> area% 49.17), oleic acid (MW:282, MF: C<sub>18</sub>H<sub>34</sub>O<sub>2</sub>, area% 8.67), palmitic acid (MW:256, MF: C<sub>16</sub>H<sub>32</sub>O<sub>2</sub>, area% 4.50), cupreol (MW:414, MF: C<sub>29</sub>H<sub>50</sub>O, area% 4.10), and pentatriacontane (MW:492, MF: C<sub>35</sub>H<sub>72</sub>, area% 2.98).

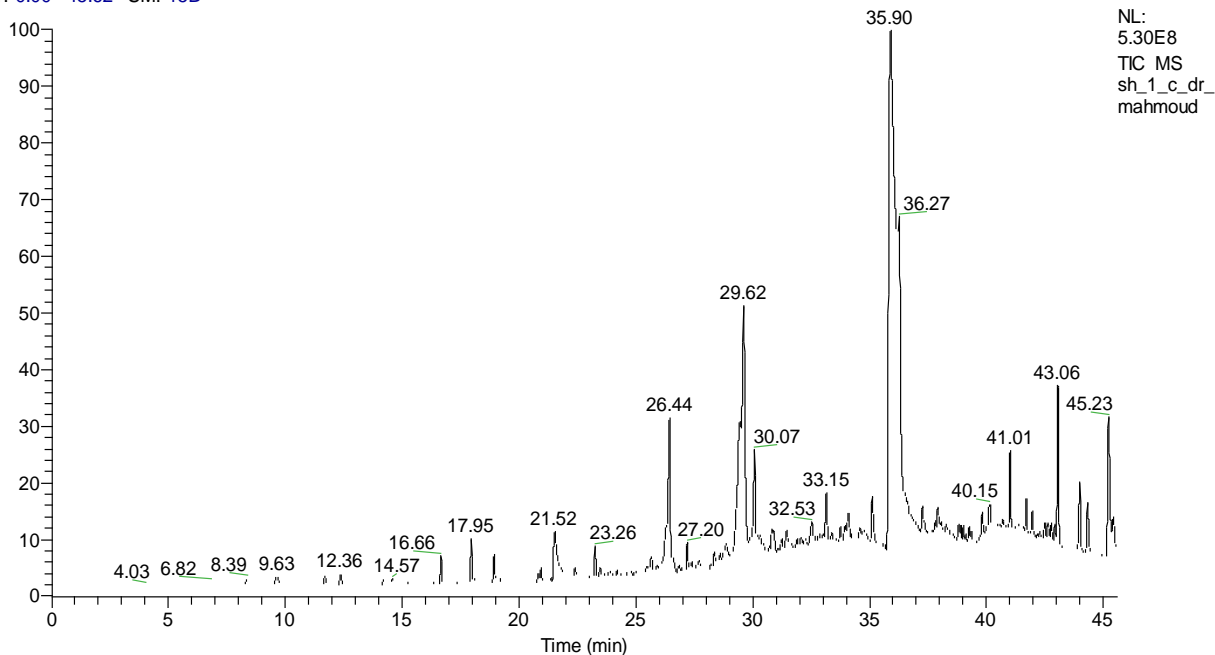
#### 3.1.2. Investigation of polar fraction using UPLC-ESI-MS/MS

For a considerable period, LC-MS has been employed in both qualitative and quantitative analyses in the realm of natural products. In the present study, we utilized reversed-phase UPLC/PDA/ESI-qTOF-MS to achieve rapid metabolite analyses and obtain better peak separations compared to traditional LC methods.

Metabolite assignments were achieved through a combination of factors, including retention time, and MS data (accurate mass, isotopic distribution, and fragmentation pattern in negative and positive ion modes) of the detected compounds.

This approach with the aid of molecular networking via the GNPS platform allowed us to annotate 44 metabolites (Fig. 9 & Fig. 10 and Table 3 & Table 4), including glycosides, carboxylic acid derivatives, lipids of triterpene derivatives, alkaloids, and flavonoid.

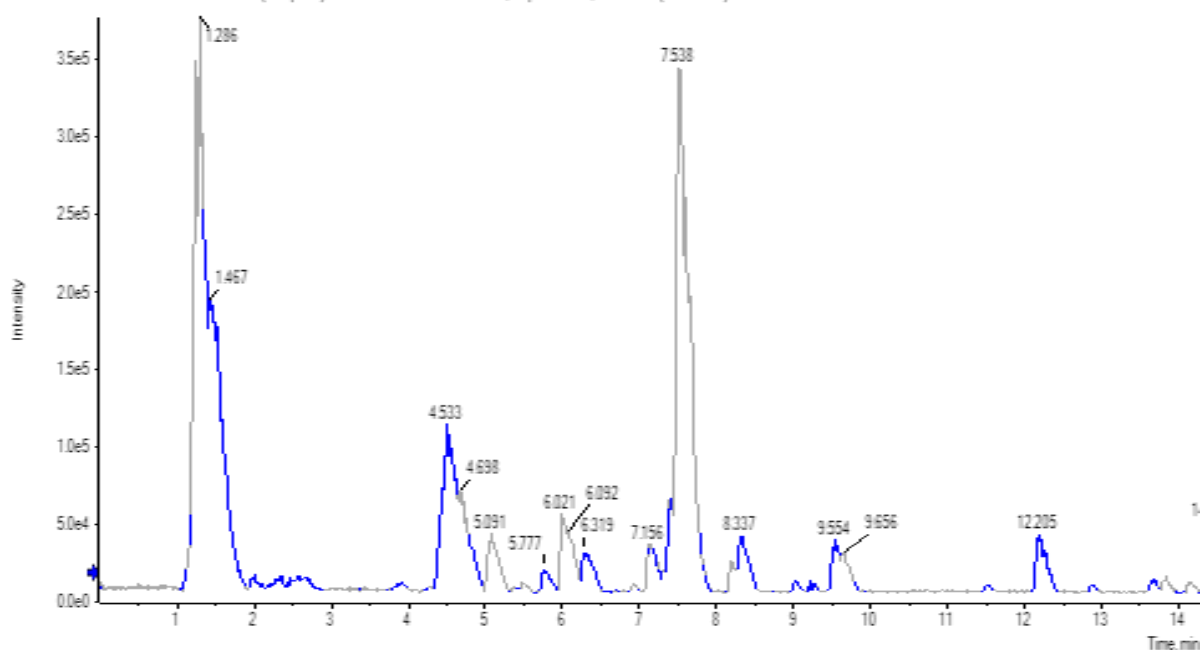
RT: 0.00 - 45.62 SM: 15B

**Fig. 8.** GC/MS analysis of the non-polar (C-Hex) fraction of *S. griseorubnes*

**Table 2.** GC-MS data of the non-polar (C-Hex) fraction of *S.griseorubens*

No.	Rt (min)	Compound Name	Mol. Weight	Mol. Formula	Area %
1	16.66	2,4-di-tert-butylphenol	206	C <sub>14</sub> H <sub>22</sub> O	0.50
2	17.95	Diethyl Phthalate	222	C <sub>12</sub> H <sub>14</sub> O <sub>4</sub>	0.79
3	18.93	2-Methylhexadecan-1-ol	256	C <sub>17</sub> H <sub>36</sub> O	0.67
4	21.52	2,4-dichlorophenoxyacetic acid	221	C <sub>8</sub> H <sub>6</sub> Cl <sub>2</sub> O <sub>3</sub>	2.29
5	23.26	1-nonadecene	266	C <sub>19</sub> H <sub>38</sub>	0.55
6	25.66	Elaidic Acid	282	C <sub>18</sub> H <sub>34</sub> O <sub>2</sub>	0.43
7	26.30-26.44	Palmitic acid	256	C <sub>16</sub> H <sub>32</sub> O <sub>2</sub>	4.50
8	27.20	<i>cis</i> -13-Eicosenoic acid	310	C <sub>20</sub> H <sub>38</sub> O <sub>2</sub>	0.49
9	29.43	Linoleic acid	280	C <sub>18</sub> H <sub>32</sub> O <sub>2</sub>	4.75
10	29.62	Oleic Acid	282	C <sub>18</sub> H <sub>34</sub> O <sub>2</sub>	8.67
11	30.07	Stearic acid	284	C <sub>18</sub> H <sub>36</sub> O <sub>2</sub>	2.43
12	30.88	hexadecadienoic acid, methyl ester	266	C <sub>17</sub> H <sub>30</sub> O <sub>2</sub>	0.62
13	32.53	Linoleic acid ethyl ester	536	C <sub>20</sub> H <sub>36</sub> O <sub>2</sub>	0.79
14	33.15	Fluroxypyr-1-methylheptyl ester	366	C <sub>15</sub> H <sub>21</sub> C <sub>12</sub> FN <sub>2</sub> O <sub>3</sub>	1.15
15	35.90-36.27	bis(2-ethylhexyl) phthalate	390	C <sub>24</sub> H <sub>38</sub> O <sub>4</sub>	49.17
16	40.15	1-Heptatriacotanol	536	C <sub>37</sub> H <sub>76</sub> O	0.46
17	41.01	Heptacosane	380	C <sub>27</sub> H <sub>56</sub>	1.31
18	43.06	Pentatriacontane	492	C <sub>35</sub> H <sub>72</sub>	2.98
19	43.99	3-Ethyl-5-(2'-ethylbutyl)octadecane			1.65
20	44.33	2-(3,4-dimethoxyphenyl)-3,5-dihydroxy-7-methoxy-4H-1-benzopyran-4-one	344	C <sub>18</sub> H <sub>16</sub> O <sub>7</sub>	1.27
21	45.23	Cupreol	414	C <sub>29</sub> H <sub>50</sub> O	4.10

BPC from DA-POS-230501-SM0246-1.wiff (sample 1) - DA-POS-230501-SM0246-1, Experiment 1, +TOF MS (50 - 1000)

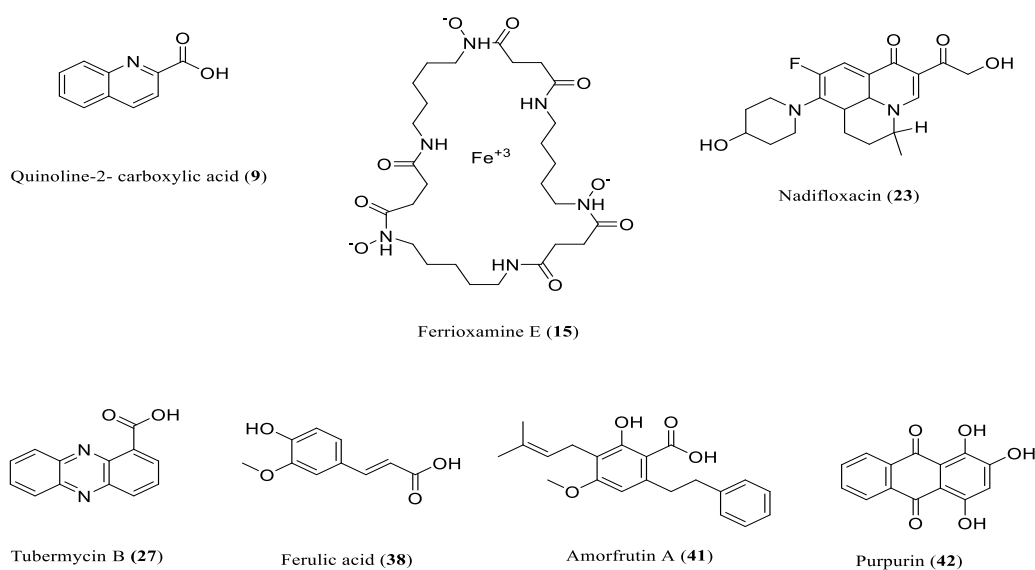
**Fig. 9.** UPLC-(+)ESI-MS chromatogram for the defatted extract of *S.griseorubens*.

**Table 3.** Positive mode of UPLC-MS data for *S. griseorubens* defatted extract.

NO.	R <sub>f</sub> (min)	m/z	Adduct	Family	Tentative Name	Mol. Formula	Fragments	Ref.
1	1.286	365	[M+Na] <sup>+</sup>	Tetralins	NCGC00169103-03	C <sub>19</sub> H <sub>18</sub> O <sub>6</sub>	150, 70	[21]
2	1.299	233	[M+H] <sup>+</sup>	<i>N</i> -phenylureas	Diuron	C <sub>9</sub> H <sub>10</sub> Cl <sub>2</sub> N <sub>2</sub> O	233, 187	[22]
3	1.31	150	[M+H] <sup>+</sup>	Purines	3-Methyladenine	C <sub>6</sub> H <sub>7</sub> N <sub>5</sub>	133	[23]
4	1.32	689	[M+Na] <sup>+</sup>	Triterpenoids	NCGC00179844-02	C <sub>36</sub> H <sub>58</sub> O <sub>11</sub>	666, 185	GNPS
5	1.35	529	[M+Na] <sup>+</sup>	Glycosides	NCGC00381225-01	C <sub>21</sub> H <sub>30</sub> O <sub>14</sub>	163, 167, 331	GNPS
6	1.457	543	[M+Na] <sup>+</sup>	<i>O</i> -acylglycosides	NCGC00384905-01	C <sub>24</sub> H <sub>40</sub> O <sub>12</sub>	543, 335	[24]
7	1.8	139	[M+H] <sup>+</sup>	Imidazolyl carboxylic acid	Urocanic acid	C <sub>6</sub> H <sub>6</sub> N <sub>2</sub> O <sub>2</sub>	53	[25]
8	1.85	449	[M+Na] <sup>+</sup>	Glucopyranoside	NCGC00380647-01	C <sub>17</sub> H <sub>30</sub> O <sub>12</sub>	426, 245	GNPS
9	2.07	174	[M+H] <sup>+</sup>	Quinoline carboxylic acid	Quinoline-2- carboxylic acid	C <sub>10</sub> H <sub>7</sub> O <sub>2</sub>	157, 173	GNPS
10	2.3	146	[M+H] <sup>+</sup>	Gamma amino acid	4-guanidinobutanoic acid	C <sub>5</sub> H <sub>11</sub> N <sub>3</sub> O <sub>2</sub>	86, 69	[26]
11	2.4	282	[M+H] <sup>+</sup>	Purine nucleosides	1-Methyladenosine	C <sub>11</sub> H <sub>15</sub> N <sub>5</sub> O <sub>4</sub>	150	[27]
12	2.51	114	[M+H] <sup>+</sup>	Alpha amino acid	Creatine	C <sub>4</sub> H <sub>7</sub> N <sub>3</sub> O	72, 57, 43	[28]
13	3.5	133	[M+H] <sup>+</sup>	Aromatic aldehyde	<i>trans</i> -Cinnamaldehyde	C <sub>9</sub> H <sub>8</sub> O	77, 55	[29]
14	3.85	391	[M+H] <sup>+</sup>	Benzoic acid esters	Bis(2-ethylhexyl) phthalate	C <sub>24</sub> H <sub>38</sub> O <sub>4</sub>	167, 149, 113	[30]
15	4.598	654	[M+H] <sup>+</sup>	Siderophores	Ferrioxamine E	C <sub>27</sub> H <sub>45</sub> FeN <sub>6</sub> O <sub>9</sub>	636, 619	[31, 32]
16	5.77	413	[M+Na] <sup>+</sup>	Phenoxyacetic acid	2-methyl-2-(3-pentadecylphenoxy)propanoic acid	C <sub>25</sub> H <sub>42</sub> O <sub>3</sub>	327	GNPS
17	6.37	211	[M+H] <sup>+</sup>	Alpha amino acid	Cyclo(leucylprolyl)	C <sub>11</sub> H <sub>18</sub> N <sub>2</sub> O <sub>2</sub>	183, 86, 70	[33]
18	7.26	245	[M-H <sub>2</sub> O+H] <sup>+</sup>	Dipeptide	Prolylphenylalanine	C <sub>14</sub> H <sub>18</sub> N <sub>2</sub> O <sub>3</sub>	154, 120, 98, 70	[34]
19	7.53	331	[M+Na] <sup>+</sup>	Methoxybenzoic acid	8-(3-methoxy-2-(methoxycarbonyl)phenyl)octanoic acid	C <sub>17</sub> H <sub>24</sub> O <sub>5</sub>	331, 298	GNPS
20	8.33	164	[M+H] <sup>+</sup>	Acetamide derivative	N-(2-Phenylethyl)acetamide	C <sub>10</sub> H <sub>13</sub> NO	103, 79	[35]
21	8.41	372	[M+H] <sup>+</sup>	Aporphine alkaloids	Duguetine N-oxide	C <sub>20</sub> H <sub>21</sub> NO <sub>6</sub>	295	[36, 37]
22	8.6	203	[M+H] <sup>+</sup>	Indole alkaloid	N-Acetyltryptamine	C <sub>12</sub> H <sub>14</sub> N <sub>2</sub> O	144	[38]
23	8.85	361	[M+H] <sup>+</sup>	Fluoroquinolone	Nadifloxacin	C <sub>19</sub> H <sub>21</sub> FN <sub>2</sub> O <sub>4</sub>	343, 214	GNPS
24	8.87	383	[M+Na] <sup>+</sup>	Glycosides	Junipediol A 8-glucoside	C <sub>16</sub> H <sub>24</sub> O <sub>9</sub>	360, 85	[39]
25	10.9	471	[M+Na] <sup>+</sup>	Glycosides	NCGC00380538-01	C <sub>21</sub> H <sub>36</sub> O <sub>10</sub>	471, 339	GNPS
26	11.3	299	[M+K] <sup>+</sup>	Naphthoquinones	2-hydroxy-3-(3-hydroxy-3-methylbutyl)naphthalene-1,4-dione	C <sub>15</sub> H <sub>16</sub> O <sub>4</sub>	281	[40]
27	11.65	225	[M+H] <sup>+</sup>	Phenazines	Tubermycin B	C <sub>13</sub> H <sub>8</sub> N <sub>2</sub> O <sub>2</sub>	224, 208, 207, 179	[41]
28	11.78	405	[M+Na] <sup>+</sup>	Cyclohexenones	Ochrephilone	C <sub>23</sub> H <sub>26</sub> O <sub>5</sub>	361	[42]
29	11.92	355	[M+Na] <sup>+</sup>	Terpene glycosides	NCGC00385387-01	C <sub>16</sub> H <sub>28</sub> O <sub>7</sub>	119, 203	GNPS
30	13.8	547	[M+Na] <sup>+</sup>	Lignan glycosides	NCGC00385320-01	C <sub>26</sub> H <sub>36</sub> O <sub>11</sub>	350, 159	GNPS

**Table 4.** Negative mode of UPLC-MS data for *S.griseorubens* defatted extract.

NO.	Rt (min)	m/z	Adduct	Family	Tentative Name	Mol. Formula	Fragments	Ref.
31	1.06	117	[M-H] <sup>-</sup>	Dicarboxylic acids	Succinic acid	C <sub>4</sub> H <sub>6</sub> O <sub>4</sub>	99, 73	[28]
32	1.1	259	[M-H] <sup>-</sup>	Monosaccharides	Alpha-D-galactose-1-phosphate	C <sub>6</sub> H <sub>13</sub> O <sub>9</sub> P	241, 139, 97, 79	[43]
33	1.15	191	[M-H] <sup>-</sup>	Tricarboxylic acids	Citric acid	C <sub>6</sub> H <sub>8</sub> O <sub>7</sub>	129, 111	[44]
34	1.16	147	[M-H] <sup>-</sup>	Hydroxy fatty acids	Citramalic acid	C <sub>5</sub> H <sub>8</sub> O <sub>5</sub>	103, 87, 85	[45]
35	1.3	133	[M-H] <sup>-</sup>	Beta hydroxy acids	(S)-2-hydroxysuccinic acid	C <sub>4</sub> H <sub>6</sub> O <sub>5</sub>	73, 71	[46]
36	1.34	341	[M-H] <sup>-</sup>	Glycosylglucose	D-(+)-Cellobiose	C <sub>12</sub> H <sub>22</sub> O <sub>11</sub>	161, 101, 97, 73	[47]
37	5.8	445	[M-H] <sup>-</sup>		Unknown			
38	6.5	193	[M-H] <sup>-</sup>	Phenolic acids	Ferulic acid	C <sub>10</sub> H <sub>10</sub> O <sub>4</sub>	133, 119	[48]
39	9.1	253	[M-H] <sup>-</sup>	Flavones	Chrysin	C <sub>15</sub> H <sub>10</sub> O <sub>4</sub>	209	[49]
40	13.1	269	[M-H] <sup>-</sup>	Flavones	Baicalein	C <sub>15</sub> H <sub>10</sub> O <sub>5</sub>	223, 139	[50]
41	16.25	339	[M-H] <sup>-</sup>	Stilbenoids	Amorfrutin A	C <sub>21</sub> H <sub>24</sub> O <sub>4</sub>	295, 211	[51]
42	16.8	255	[M-H] <sup>-</sup>	Hydroxyanthraquinones	Purpurin	C <sub>14</sub> H <sub>8</sub> O <sub>5</sub>	183, 171	[52]
43	20.5	253	[M-H] <sup>-</sup>	Fatty acids	Palmitoleic acid	C <sub>16</sub> H <sub>30</sub> O <sub>2</sub>	93	[53]
44	21.0	279	[M-H] <sup>-</sup>	Fatty acids	Linoleic acid	C <sub>18</sub> H <sub>32</sub> O <sub>2</sub>	261, 111	[54]

**Fig. 10.** Chemical structure of selected metabolites identified from *S.griseorubens* defatted extract.

### 3.2. In Vitro Biological Activities

#### 3.2.1 Antioxidant Activity:

The assessment of the antioxidant capacity of the ethyl acetate extract derived from *S. griseorubens* was conducted employing the (DPPH) technique [55].

The resultant values, denoted by an IC<sub>50</sub> of 55.97 µg/ml for the extract (Fig. 11) were compared with ascorbic acid, serving as the positive control (Fig. 12).

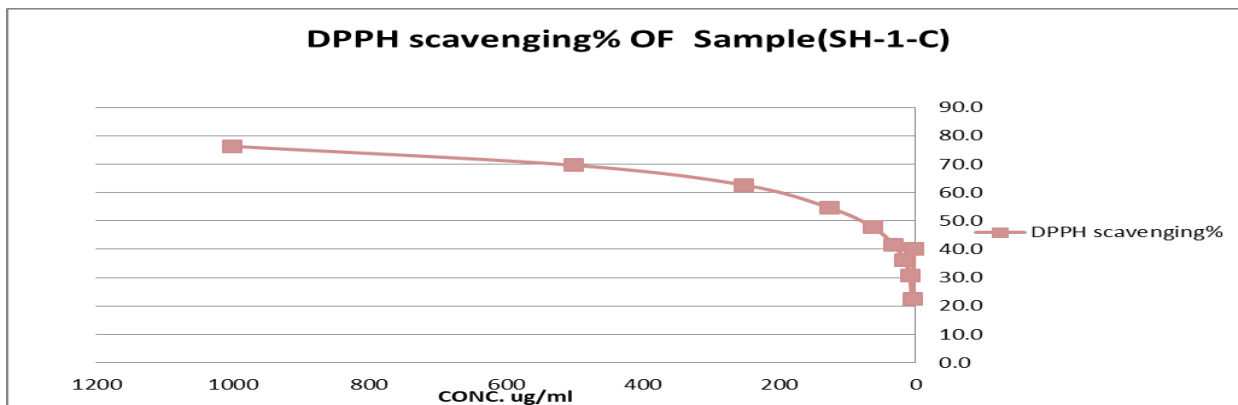


Fig. 11. Antioxidant activity of *S.griseorubnes* crude extract

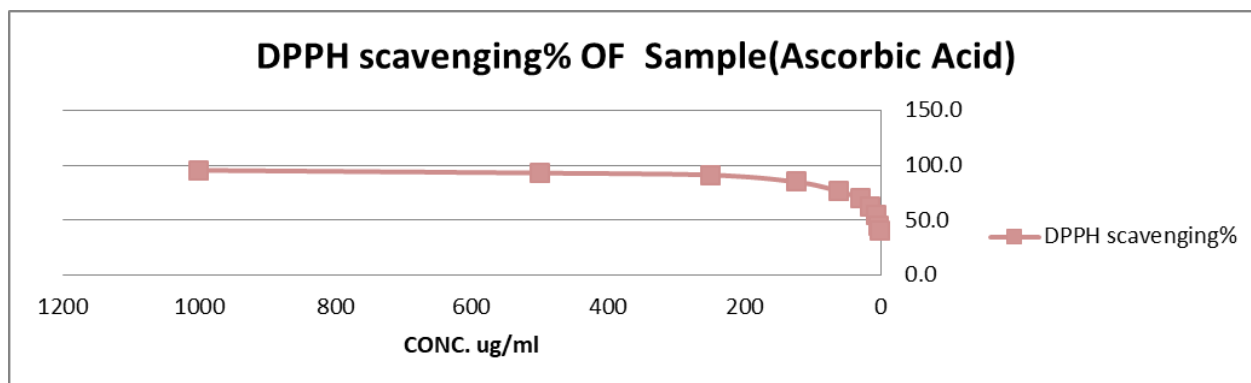


Fig. 12. Antioxidant activity for ascorbic acid as a positive control

### 3.2.2. Anticancer Activity

The IC<sub>50</sub> value for the comprehensive extract derived from *S. griseorubnes* when subjected to breast cancer cell lines (MCF7) was calculated at several concentrations using the MTT protocol. It showed an

IC<sub>50</sub> value of 343.34 µg/mL, in contrast with doxorubicin, serving as a reference (Fig. 13, Fig. 14, and Fig. 15). While the crude extract displayed relatively low activity against MCF7, it manifested a noteworthy capability to hinder the proliferation of MCF7 cancer cells.

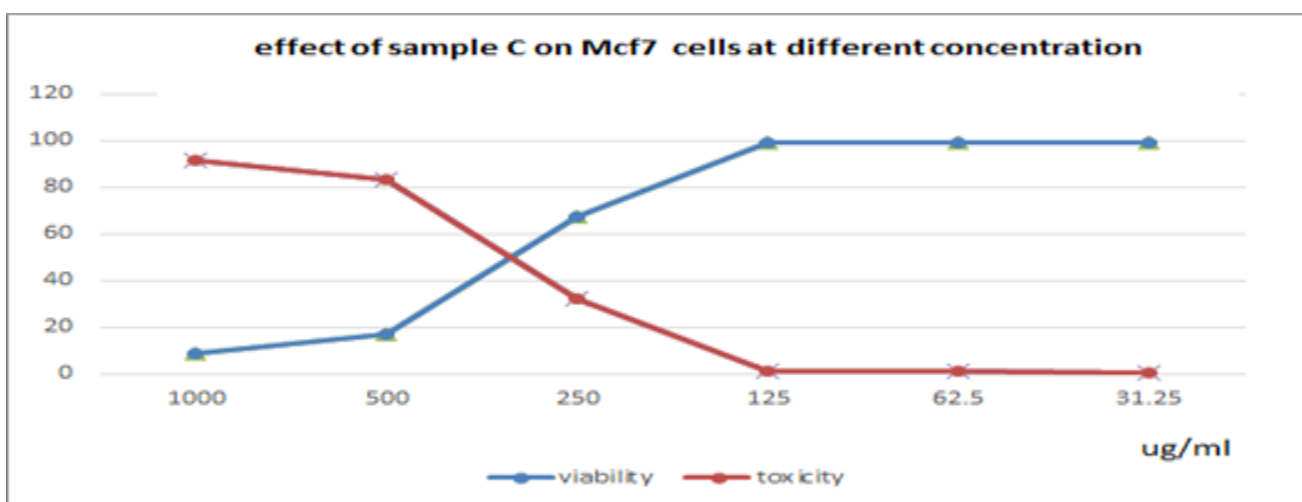


Fig. 13. Effect of *S.griseorubnes* crude extract on MCF7 cells at different concentrations

### Effect of sample C on MCF7 cells at different concentration

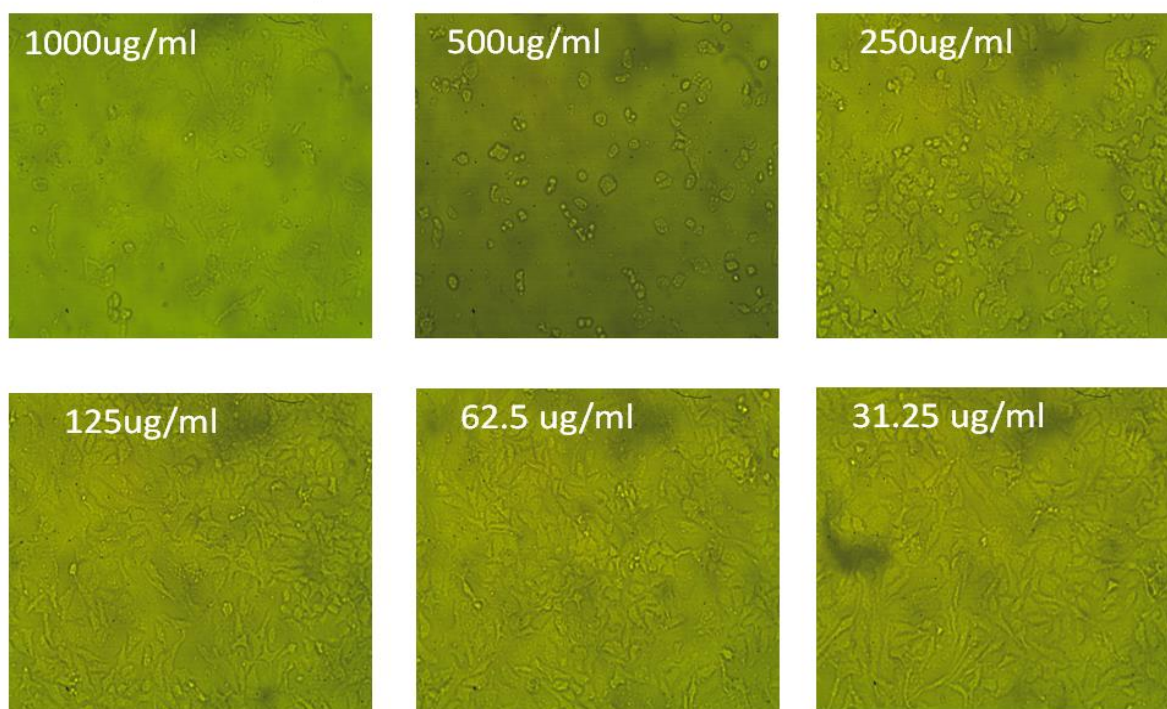


Fig. 14. Effect of *S.griseorubnes* crude extract on MCF7 cells at different concentrations

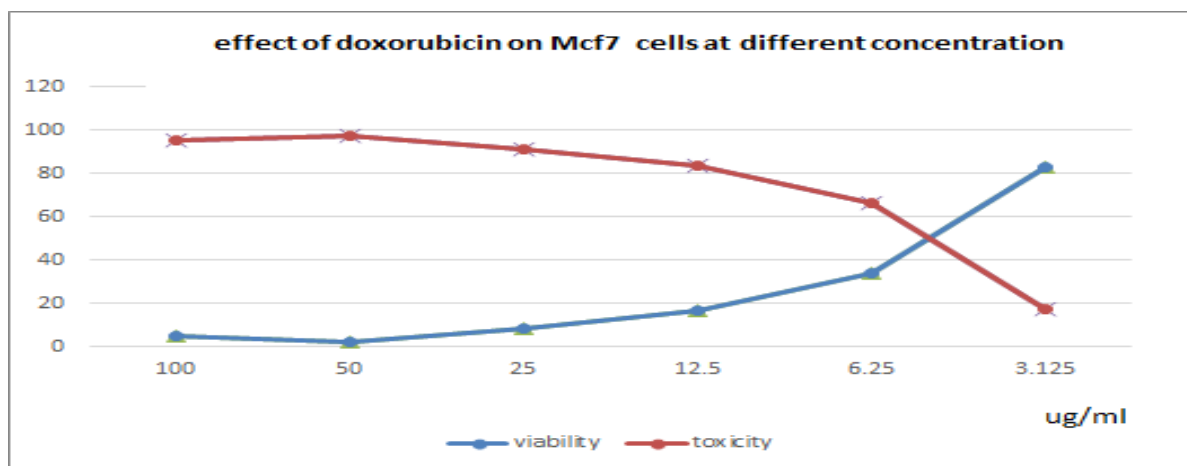


Fig. 15. Effect of doxorubicin as control positive on MCF7 cells at different concentrations

#### 4. Discussion

Actinomycetes play a crucial role in biotechnology and industry. The isolation and characterization of actinomycetes hold significance for the production of natural colors with industrial applications [56]. Various pigments are regularly employed in medicine, pharmaceutical industries, and cosmetics, and these pigments originate from diverse microorganisms,

encompassing bacterial and fungal species. Likewise, our study reveals the antioxidant and anticancer properties and natural pigment-producing capabilities of actinomycetes, suggesting potential applications in various industries [57].

In our current investigation, a total of 94 actinomycetes were isolated, and subsequent selection focused on five actinomycetes with notable pigment-producing capabilities. Following an assessment of diffusion abilities, *S. griseorubens* emerged as the most promising isolate, warranting further

investigation. The pigment-producing capacity of *S. griseorubens* underwent testing on both solid and liquid media. Morphological characteristics were documented in accordance with the International *Streptomyces* Project (ISP) guidelines, revealing prolific growth of aerial and vegetative mycelium on starch nitrate medium, yeast extract-malt extract medium (ISP-2), and oatmeal agar (ISP-3). Several researchers have previously reported on the prevalence and dominance of *Streptomyces* isolates among actinomycetes across diverse soil types [58-60]. The morphological analysis of *S. griseorubens* revealed the development of an orange-colored reverse pigment on both starch nitrate and ISP-2 media. The acquisition of soil samples and the isolation of actinomycetes were guided by the methodology outlined by Selvameenal et al., affirming the existence of actinomycetes with notable pigment-producing capabilities and antimicrobial activities. Numerous studies have additionally documented the isolation of actinomycetes from desert soil [61-63].

According to reports, the rhizosphere soil serves as an abundant reservoir of microorganisms, particularly actinomycetes, possessing a substantial population capable of generating numerous bioactive compounds. Actinomycetes populations are prevalent in rhizosphere soil and are extensively distributed within plant root systems [64-66].

In this current study, *S. griseorubens* exhibited prolific growth with various carbon sources, including starch, lactose, dextrose, mannitol, maltose, and fructose. Among these, starch proved to be the most favorable carbon source, while ammonium nitrate demonstrated optimal nitrogen support. Additionally, *S. griseorubens* demonstrated hydrolytic activities on lipids, casein, starch, urea, and gelatin but lacked cellulose-degrading capabilities. Notably, pigment production peaked at pH 5 on the 8<sup>th</sup> day of the incubation period, contrary to findings in other studies that observed maximum melanin activity at neutral pH 7, with a decline at higher pH values [67]. Our results aligned with Mortazavian et al. [68], who reported that optimal yellow pigment assembly occurred at initial pH values between 3.0 and 3.5, while the finest results for red pigment assembly were achieved at pH levels between 7.0 and 7.5.

For taxonomic classification, the AUMC B-519 strain underwent genetic sequencing through

polymerase chain reaction (PCR), subsequent sequencing, and BLAST-based analysis. Phylogenetic analysis of the 16S rRNA gene sequence indicated a high similarity between AUMC B-519 and *S. griseorubens*, with a match of 99.79%. The phylogenetic tree (Fig. 3) was constructed using the neighbour-joining method with 1000 bootstrap in MEGA6 [69], with *Bacillus thuringiensis* strain ATCC 10792 (NR\_114581) as the outgroup branch. The 16S rRNA gene sequence of strain MPT42 was deposited in GenBank (NCBI) under the accession number [OQ909101](#).

In terms of metabolomic profiling, the GC-MS analysis (Fig. 8) revealed a discernible prevalence of a distinct group of compounds within the non-polar fraction. As indicated in

Table 2, twenty-one metabolites, the majority of which have been identified here for the first time from *S. griseorubens* comprise a noteworthy presence of fatty acid derivatives. Among these, oleic acid (MW: 282, MF: C<sub>18</sub>H<sub>34</sub>O<sub>2</sub>, area% 8.67), known as 9,12-octadecadienoic acid, emerged as a prominent constituent. This polyunsaturated fatty acid, found in both animals and various vegetable oils, offers a multitude of health benefits. Its attributes encompass a diverse range of antibiotic functions, a reduction in the risk of heart attacks and atherosclerosis, and facilitation in cancer prevention [70]. Palmitic acid (MW: 256, MF: C<sub>16</sub>H<sub>32</sub>O<sub>2</sub>, area % 4.50), also referred to as hexadecanoic acid, was detected. This compound has been previously documented for its antioxidant and anticancer properties [71].

Furthermore, elaidic acid, *cis*-13-eicosenoic acid, linoleic acid, and stearic acid were also identified.

On the other hand, the UPLC-MS/MS data of the defatted extract of *S. griseorubens* is illustrated in Fig. 9 and detailed in Table 3 and Table 4. This analysis involved the scrutiny of 44 metabolites, tentatively identified for the first time from both positive and negative modes, showcasing a diversity of compound classes. Notably, these include glycosides, carboxylic acid derivatives, lipids of triterpene derivatives, alkaloids, and flavonoids. Additionally, fatty acid derivatives, as depicted in Fig. 10, contribute to the comprehensive profile of metabolites identified in this investigation.

From the UPLC(+)-ESI-MS/MS Table 3, we tentatively identified 30 metabolites according to the accurate mass, isotopic distribution, and fragmentation

pattern with the assistance of GNPS and comparing with the authentic data. For instance, one of the prominently identified compounds from the positive ion mode was the cyclic trihydroxamate siderophore ferrioxamine E (**15**). It displayed  $[M+H]^+$  at  $m/z$  654 ( $C_{27}H_{45}FeN_6O_9$ )<sup>+</sup>. Previous studies have highlighted distinctive cleavage patterns in the cyclized trihydroxamate, setting it apart from structurally analogous linear trihydroxamates [32]. The anticipated ions from these cleavage events were duly detected in the MS<sup>2</sup> spectra of (**15**), specifically at  $m/z$  values of 636 and 619. To the best of our knowledge, trihydroxamate siderophores are produced by synthetases independent of nonribosomal peptide synthesis (NRS) and typically incorporate blocks of N-hydroxy-N-succinyl-cadaverine [72].

In the negative ionization modes UPLC(-)ESI-MS/MS Table 4, the chromatogram was partitioned into four distinct segments, delineating metabolite classes, namely organic acids, cinnamates, flavonoids, and fatty acids. Notably, the latter exhibits a proclivity for ionization under negative ionization conditions. Phenolics such as ferulic acid (**38**), amorfrutin A (**41**), purpurin (**42**), characterized by their relatively polar nature and the presence of phenol groups in their molecular structures, align with expectations by readily undergoing ionization in the negative ionization mode.

Regarding the *in vitro* biological efficacy of the ethyl acetate extract obtained from *S. griseorubens*, both antioxidant and anticancer activities were scrutinized. The obtained results reveal an IC<sub>50</sub> value of 55.97 µg/mL for the antioxidant activity assessed through the DPPH method. Simultaneously, the IC<sub>50</sub> value for the same extract against breast cancer cell lines (MCF7), evaluated using the MTT assay, was determined to be 343.34 µg/mL.

## 5. Conclusion

In summary, this study delves into the specific focus on *S. griseorubens* isolated from diverse soil sites across Egypt. The investigation involved a comprehensive exploration comprising subsequent metabolomic profiling through GC-MS and UPLC-MS coupled with QTOF-MS. Notably, a plethora of compounds, many of which were identified for the first time from *S. griseorubens*.

The metabolomic analysis, employing GC-MS, disclosed 21 compounds, while UPLC-MS revealed a

more expansive profile of 44 compounds with diverse structures. This intricate chemical diversity provides valuable insights into the complex metabolic pathways and compounds synthesized by *S. griseorubens*. Concurrently, the ethyl acetate extract was subjected to antioxidant and anticancer activity assessments. The extract exhibited moderate anticancer activity against the MCF7 cell line and a restrained effect in DPPH scavenging, with MIC values of 343.34 and 55.97 µg/mL, respectively.

This study conclusively positions *S. griseorubens* as a promising reservoir of bioactive compounds. The metabolomic profiling not only contributes to understanding its pharmacological properties but also serves as a foundation for further biomedical investigations. The identified metabolites emphasize the novelty and potential of *S. griseorubens* in expanding our repertoire of bioactive molecules with therapeutic applications.

## Conflicts of interest

The authors declare that there are no conflicts of interest.

## References

- Asmaey, M.A., Unravelling the Secrets of  $\alpha$ -Pyrone from *Aspergillus* Fungi: A Comprehensive Review of Their Natural Sources, Biosynthesis, and Biological Activities. *Chem. Biodivers.*, **2023**. e202301185.
- Asmaey, M.A., et al., Ochraceopyronide, a Rare  $\alpha$ -Pyrone-C-lyxofuranoside from a Soil-Derived Fungus *Aspergillus ochraceopetaliformis*. *Molecules*, **2021**, *26*, 3976. <https://doi.org/10.3390/molecules26133976>.
- El-Naggar, N.E.-A., *Streptomyces*-based cell factories for production of biomolecules and bioactive metabolites, in *Microbial Cell Factories Engineering for Production of Biomolecules*. 2021, Elsevier. p. 183-234.
- Yang, W., et al., Bioactive Secondary Metabolites from Marine *Streptomyces griseorubens* f8: Isolation, Identification and Biological Activity Assay. *Journal of Marine Science and Engineering*, **2021**, *9*, 978.
- Prasad, P., T. Singh, and S. Bedi, Characterization of the cellulolytic enzyme produced by *Streptomyces griseorubens* (Accession No. AB184139) isolated from Indian soil. *Journal of King Saud University-Science*, **2013**, *25*, 245-250.
- Leaves, L. and L. Leaves, Antioxidant activity by DPPH radical scavenging method of *ageratum conyzoides*. *American Journal of Ethnomedicine*, **2014**, *1*, 244-249.
- Blunt, J.W., et al., Marine natural products. *Natural product reports*, **2018**, *35*, 8-53.
- Atanasov, A.G., et al., Natural products in drug discovery: Advances and opportunities. *Nature reviews Drug discovery*, **2021**, *20*, 200-216.
- McPherson, M.R., et al., Isolation and analysis of microbial communities in soil, rhizosphere, and roots in perennial grass experiments. *JoVE*

- (*Journal of Visualized Experiments*), **2018**. e57932.
10. Jastaniah, S., et al., Inhibition of some human bacterial pathogens using *Streptomyces* sp. Sd5 obtained from soil sample from Jeddah. *Journal of Experimental Biology and Agricultural Sciences*, **2019**, *7*, 222-232.
  11. El Karkouri, A., S.A. Assou, and M. El Hassouni, Isolation and screening of actinomycetes producing antimicrobial substances from an extreme Moroccan biotope. *The Pan African Medical Journal*, **2019**, *33*.
  12. Chakraborty, B., et al., *Streptomyces filamentosus* strain KS17 isolated from microbiologically unexplored marine ecosystems exhibited a broad spectrum of antimicrobial activity against human pathogens. *Process Biochemistry*, **2022**, *117*, 42-52.
  13. Chauhan, A. and T. Jindal, Biochemical and molecular methods for bacterial identification. *Microbiological methods for environment, food and pharmaceutical analysis*, **2020**, 425-468.
  14. Zimbro, M., et al., Difco & BBL manual of microbiological culture media. *Becton, Dickinson and Company, Maryland*, **2009**.
  15. White, T.J., et al., Amplification and direct sequencing of fungal ribosomal RNA genes for phylogenetics. *PCR protocols: a guide to methods and applications*, **1990**, *18*, 315-322.
  16. Bayram, S., et al., Bioproduction, structure elucidation and in vitro antiproliferative effect of eumelanin pigment from *Streptomyces parvus* BSB49. *Arch. Microbiol.*, **2020**, *202*, 2401-2409.
  17. Abd El-Kareem, M.S., et al., Application of GC/EIMS in combination with semi-empirical calculations for identification and investigation of some volatile components in basil essential oil. *International Journal of Analytical Mass Spectrometry and Chromatography*, **2016**, *4*, 14-25.
  18. Hegazy, M.M., et al., Biological and chemical evaluation of some African plants belonging to *Kalanchoe* species: Antitrypanosomal, cytotoxic, antitopoisomerase I activities and chemical profiling using ultra-performance liquid chromatography/quadrupole-time-of-flight mass spectrometer. *Pharmacogn. Mag.*, **2021**, *17*, 6-15.
  19. Fayek, N.M., et al., Comparative metabolite profiling of four citrus peel cultivars via ultra-performance liquid chromatography coupled with quadrupole-time-of-flight-mass spectrometry and multivariate data analyses. *J. Chromatogr. Sci.*, **2019**, *57*, 349-360.
  20. Tolosa, L., M.T. Donato, and M.J. Gómez-Lechón, General cytotoxicity assessment by means of the MTT assay. *Protocols in in vitro hepatocyte research*, **2015**, 333-348.
  21. Abrams, R.P., et al., Therapeutic candidates for the Zika virus identified by a high-throughput screen for Zika protease inhibitors. *Proceedings of the National Academy of Sciences*, **2020**, *117*, 31365-31375.
  22. Temgoua, R.C., et al., Simulation of the environmental degradation of diuron (herbicide) using electrochemistry coupled to high resolution mass spectrometry. *Electrochimica Acta*, **2020**, *352*, 136485.
  23. Stoller, C., et al., 3-Methyladenine from the marine sponge *Topsentia genitrix*. *J. Nat. Prod.*, **1988**, *51*, 383-384.
  24. Yan, H., et al., Integrative Metabolome and Transcriptome Analysis Reveals the Regulatory Network of Flavonoid Biosynthesis in Response to MeJA in *Camellia vietnamensis* Huang. *Int. J. Mol. Sci.*, **2022**, *23*, 9370.
  25. Evans, D.R., et al., The biosynthesis of nikkomycin X from histidine in *Streptomyces tendae*. *Tetrahedron Lett.*, **1995**, *36*, 2351-2354.
  26. Carey, J., et al., An isotopic ratio outlier analysis approach for global metabolomics of biosynthetically talented actinomycetes. *Metabolites*, **2019**, *9*, 181.
  27. Hauenschild, R., et al., The reverse transcription signature of N-1-methyladenosine in RNA-Seq is sequence dependent. *Nucleic Acids Res.*, **2015**, *43*, 9950-9964.
  28. Abdelrahman, S.M., et al., Metabolomic profiling and molecular networking of nudibranch-associated *Streptomyces* sp. SCSIO 001680. *Molecules*, **2022**, *27*, 4542.
  29. Lončar, M., et al., Coumarins in food and methods of their determination. *Foods*, **2020**, *9*, 645.
  30. Driche, E.H., et al., A new *Streptomyces* strain isolated from Saharan soil produces di-(2-ethylhexyl) phthalate, a metabolite active against methicillin-resistant *Staphylococcus aureus*. *Annals of microbiology*, **2015**, *65*, 1341-1350.
  31. Ueki, M., et al., Nocardamin production by *Streptomyces avermitilis*. *Actinomycetologica*, **2009**, *23*, 34-39.
  32. Sidebottom, A.M., J.A. Karty, and E.E. Carlson, Accurate mass MS/MS/MS analysis of siderophores ferrioxamine B and E1 by collision-induced dissociation electrospray mass spectrometry. *Journal of the American Society for Mass Spectrometry*, **2015**, *26*, 1899-1902.
  33. Djebbah, F.Z., et al., Isolation and characterization of novel *Streptomyces* strain from Algeria and its in-vitro antimicrobial properties against microbial pathogens. *Journal of Infection and Public Health*, **2021**, *14*, 1671-1678.
  34. Betancur, L.A., et al., Cyclic tetrapeptides from the marine strain *Streptomyces* sp. PNM-161a with activity against rice and yam phytopathogens. *The Journal of Antibiotics*, **2019**, *72*, 744-751.
  35. Shaaban, K.A., et al., Venturicidin C, a new 20-membered macrolide produced by *Streptomyces* sp. TS-2-2. *The Journal of antibiotics*, **2014**, *67*, 223-230.
  36. Paz, W.H., et al., Structure-based molecular networking for the target discovery of oxahomoaporphine and 8-oxohomoaporphine alkaloids from *Duguetia surinamensis*. *J. Nat. Prod.*, **2019**, *82*, 2220-2228.
  37. Silva, D.B.d., et al., Chemical constituents of the underground stem bark of *Duguetia furfuracea* (Annonaceae). *J. Braz. Chem. Soc.*, **2007**, *18*, 1560-1565.
  38. Zhang, W., et al., Antibacterial activity composition of the fermentation broth of *Streptomyces djakartensis* NW35. *Molecules*, **2013**, *18*, 2763-2768.
  39. Comte, G., et al., Three phenylpropanoids from *Juniperus phoenicea*. *Phytochemistry*, **1997**, *44*, 1169-1173.
  40. Hamama, W.S., A.E.D.E. Hassanien, and H.H. Zoorob, Advanced Routes in Synthesis and Reactions of Lawsonsone Molecules (2-Hydroxynaphthalene-1, 4-dione). *J. Heterocycl. Chem.*, **2017**, *54*, 2155-2196.
  41. Cheng, C., et al., Strepoxazine A, a new cytotoxic phenoxazin from the marine sponge-derived

- bacterium *Streptomyces* sp. SBT345. *Tetrahedron Lett.*, **2016**, *57*, 4196-4199.
42. Kim, H.Y., et al., Metabolomic and transcriptomic comparison of solid-state and submerged fermentation of *Penicillium expansum* KACC 40815. *PLoS One*, **2016**, *11*, e0149012.
  43. Pu, J., et al., The use of metabolomics to reveal differences in functional substances of milk whey of dairy buffaloes raised at different altitudes. *Food Funct.*, **2021**, *12*, 5440-5450.
  44. Abdel-Haliem, M., et al., Characterization of *Streptomyces* isolates causing colour changes of mural paintings in ancient Egyptian tombs. *Microbiol. Res.*, **2013**, *168*, 428-437.
  45. Apel, C., et al., Metabolic adjustments in response to ATP spilling by the small DX protein in a *Streptomyces* strain. *Frontiers in Cell and Developmental Biology*, **2023**, *11*, 1129009.
  46. Amorisco, A., et al., Identification of low molecular weight organic acids by ion chromatography/hybrid quadrupole time-of-flight mass spectrometry during Uniblu-A ozonation. *Rapid Commun. Mass Spectrom.*, **2013**, *27*, 187-199.
  47. Planckaert, S., et al., Identification of novel rothibin analogues in *Streptomyces* scabies, including discovery of its biosynthetic gene cluster. *Microbiology Spectrum*, **2021**, *9*, 10.1128/spectrum.00571-21.
  48. Asmaey, M.A., et al., Chemical constituents from *Colchicum palaestinum* (Baker) C. Archer with the assessment of its antioxidant, wound scratch, and tyrosinase repressive potential. *S. Afr. J. Bot.*, **2023**, *157*, 209-218.
  49. Pingili, R.B., et al., A comprehensive review on hepatoprotective and nephroprotective activities of chrysin against various drugs and toxic agents. *Chem. Biol. Interact.*, **2019**, *308*, 51-60.
  50. Gokhale, M., et al., Isolation of bio-molecule Baicalein (5, 6, 7-Trihydroxy flavone) from root of *Oroxylum indicum* L. Vent and its prospective interaction with COVID-19 Viral S-Protein Receptor Binding Domain. *Research Journal of Pharmacy and Technology*, **2022**, *15*, 5050-5056.
  51. Muharini, R., et al., Antibacterial and cytotoxic phenolic metabolites from the fruits of *Amorpha fruticosa*. *J. Nat. Prod.*, **2017**, *80*, 169-180.
  52. Singh, J., et al., Purpurin: A natural anthraquinone with multifaceted pharmacological activities. *Phytother. Res.*, **2021**, *35*, 2418-2428.
  53. Shalabi, A. and D.M. Eskander, Isolation of secondary metabolites from marine *Streptomyces* sparsus ASD203 and evaluation its bioactivity. *Egyptian Journal of Chemistry*, **2022**, *65*, 539-547.
  54. Çetinkaya, S., et al., Secondary metabolites of an of *Streptomyces* griseorubens isolate are predominantly pyrrole-and linoleic-acid like compounds. *Journal of Oleo Science*, **2020**, *69*, 1273-1280.
  55. El-Tantawy, H.M., A.R. Hassan, and H.E. Taha, Anticancer Mechanism of the Non-polar Extract from *Echium angustifolium* Mill. Aerial Parts in Relation to Its Chemical Content. *Egyptian Journal of Chemistry*, **2022**, *65*, 17-26.
  56. Zhang, W., et al., The screening of antimicrobial bacteria with diverse novel nonribosomal peptide synthetase (NRPS) genes from South China Sea sponges. *Marine biotechnology*, **2009**, *11*, 346-355.
  57. Selvakumar, P., et al., Isolation and characterization of melanin pigment from *Pleurotus cystidiosus* (telomorph of *Antromycopsis macrocarpa*). *World Journal of Microbiology and Biotechnology*, **2008**, *24*, 2125-2131.
  58. Mansour, S.R., The occurrence and distribution of soil actinomycetes in Saint Catherine area, South Sinai, Egypt. *Pakistan Journal of Biological Sciences*, **2003**, *6*, 721-728.
  59. Peela, S., V.B. Kurada, and R. Terli, Studies on antagonistic marine actinomycetes from the Bay of Bengal. *World journal of microbiology and biotechnology*, **2005**, *21*, 583-585.
  60. Vijayakumar, R., et al., Studies on the diversity of actinomycetes in the Palk Strait region of Bay of Bengal, India. *Actinomycetologica*, **2007**, *21*, 59-65.
  61. Selvameenal, L., M. Radhakrishnan, and R. Balagurunathan, Antibiotic pigment from desert soil actinomycetes; biological activity, purification and chemical screening. *Indian journal of pharmaceutical sciences*, **2009**, *71*, 499.
  62. Manikkam, R., et al., Effect of critical medium components and culture conditions on antitubercular pigment production from novel *Streptomyces* sp D25 isolated from Thar desert, Rajasthan. *Journal of Applied Pharmaceutical Science*, **2015**, *5*, 015-019.
  63. Saker, R., et al., *Prausserella isguenensis* sp. nov., a halophilic actinomycete isolated from desert soil. *International journal of systematic and evolutionary microbiology*, **2015**, *65*, 1598-1603.
  64. Atalan, E., et al., Biosystematic studies on novel streptomycetes from soil. *Antonie van Leeuwenhoek*, **2000**, *77*, 337-353.
  65. Sembiring, L., A.C. Ward, and M. Goodfellow, Selective isolation and characterisation of members of the *Streptomyces violaceusniger* clade associated with the roots of *Paraserianthes falcataria*. *Antonie van Leeuwenhoek*, **2000**, *78*, 353-366.
  66. Ouhdouch, Y., M. Barakate, and C. Finance, Actinomycetes of Moroccan habitats: isolation and screening for antifungal activities. *European Journal of Soil Biology*, **2001**, *37*, 69-74.
  67. Glazer, A.N., Structure and molecular organization of the photosynthetic accessory pigments of cyanobacteria and red algae. *Molecular and cellular biochemistry*, **1977**, *18*, 125-140.
  68. Mortazavian, S., A. Saber, and D.E. James, Optimization of photocatalytic degradation of acid blue 113 and acid red 88 textile dyes in a UV-C/TiO<sub>2</sub> suspension system: application of response surface methodology (RSM). *Catalysts*, **2019**, *9*, 360.
  69. Yellamanda, B., et al., Extraction and bioactive profile of the compounds produced by *Rhodococcus* sp. VLD-10. *3 Biotech*, **2016**, *6*, 1-9.
  70. Fahmy, N.M. and A.M. Abdel-Tawab, Isolation and characterization of marine sponge-associated *Streptomyces* sp. NMF6 strain producing secondary metabolite (s) possessing antimicrobial, antioxidant, anticancer, and antiviral activities. *Journal of Genetic Engineering and Biotechnology*, **2021**, *19*, 1-14.
  71. Bharath, B., et al., Evaluation of the anticancer potential of Hexadecanoic acid from brown algae *Turbinaria ornata* on HT-29 colon cancer cells. *Journal of Molecular Structure*, **2021**, *1235*, 130229.

72. Barry, S.M. and G.L. Challis, Recent advances in siderophore biosynthesis. *Curr. Opin. Chem. Biol.*, **2009**, *13*, 205-215.